A phonon laser

K. Vahala[*][†], M. Herrmann, S. Knünz, V. Batteiger, G. Saathoff, T. W. Hänsch and Th. Udem[†]

Red-detuned laser pumping of an atomic resonance will cool the motion of an ion or atom. The complementary regime of blue-detuned pumping is investigated in this work using a single, trapped Mg^{+} ion interacting with two laser beams, tuned above and below resonance. Widely thought of as a regime of heating, theory and experiment instead show that stimulated emission of centre-of-mass phonons occurs, providing saturable amplification of the motion. A threshold for transition from thermal to coherent oscillating motion has been observed, thus establishing this system as a mechanical analogue to an optical laser—a phonon laser. Such a system has been sought in many different physical contexts.

The control of atoms and ions by optical forces has enabled a wide range of remarkable scientific discoveries, including realizations for control of quantum information[1,2], production of exotic quantum states[3,4] and unprecedented leaps in metrology[3]. The effect of optical forces on the centre-of-mass motion of atoms is reversed by switching the laser detuning relative to an absorption-line centre. For example, dispersive optical forces are conservative and form attractive (red-detuned) or repulsive (blue-detuned) potentials[5]. Scattering forces, on the other hand, remove energy (red-detuned) and thereby cool[6–9]; or these forces add energy (blue-detuned) to the centre of mass motion[10]. The latter regime, commonly referred to as heating, has been of much less interest in the field of optical manipulation and control of ions and atoms. Nonetheless, early work showed that heating phenomena can be complex, and include multistability, and, surprisingly, the appearance of limit cycles in the ion motion[11–13]. Two, recent developments have refocused attention on this regime. First, velocity bunching has been observed in [88]Sr neutral atoms that interact over a fixed time interval with a blue-detuned pump in a magneto-optical trap[14,15]. A theory for this behaviour identifies a velocity feedback mechanism associated with the blue-detuned scattering force[14,15]. Second, parallels noted between ion studies and cavity optomechanics[16], wherein the parametric instability leads to mechanical amplification[17], further suggest that this regime of ion motion contains unexplored subtleties. It is shown here that, as opposed to heating, this regime is one of stimulated emission of phonons, providing amplification to the centre-of-mass motion. In analogy with a laser[18,19], the system functions like a Van der Pol oscillator[19,20] subject to a threshold condition and amplification saturation. There has been considerable interest in the possibility of phonon laser or maser action for many years. A wide range of systems have been analysed theoretically including ions[21], semiconductors[22], nanomechanics[23], nanomagnets[24] and others[25]. In addition, experimental evidence of phonon amplification, a pre-requisite to phonon laser action, has been reported in cryogenic Al$_2$O$_3$:Cr^{3+}(refs 26–28) and Al$_2$O$_3$:V^{4+} (ref. 29) as well as semiconductor superlattices[30]. Using a single, cooled Mg^{+} ion[31] within a Paul trap[32], observations of phonon laser action are presented and shown to be in excellent agreement with theory. Overall, the remarkable control possible in experimental trapped-ion systems makes this an interesting system in which to study phonon laser physics.

The ion resides in a harmonic trap with secular frequency Ω_0, and its motion is first considered semi-classically and later from a quantum viewpoint. The limit of unresolved motional sidebands (weak-binding regime[10]) is assumed as this case is studied experimentally. The system (Fig. 1a) features a cooling beam of intensity i_c at frequency ω_c, and a beam defined as the 'amplification' beam of intensity i_a at frequency ω_a. Each beam induces a scattering force[33] by interaction with the atomic dipole (transition frequency ω_0 and linewidth γ). The ion velocity, v, satisfies the following nonlinear oscillator equation driven by $\chi(t)$, a white-noise Langevin function that accounts for several sources of noise including spontaneous emission.

$$\ddot{v} + \left[\kappa(v)i_c - g(v)i_a\right]\dot{v} + \Omega_0^2 v = \dot{\chi}(t) \tag{1}$$

The derivation of this equation and the functional forms for $g(v)$ and $\kappa(v)$ are provided in the Supplementary Information. When $\Delta\omega_c \equiv \omega_c - \omega_0 < 0$ (red-detuned for cooling) and $\Delta\omega_a \equiv \omega_a - \omega_0 > 0$, $\kappa(v)$ and $g(v)$ are positive for 'small signal' motion ($v \approx 0$). $\kappa(v)i_c$ is an optical damping term, which for effective cooling (and $i_a = 0$), is the dominant source of damping. The term $g(v)i_a$, on the other hand, represents mechanical amplification (negative damping), later shown to result from stimulated emission of phonons. Intuitively, it results because a small, positive change in ion velocity will Doppler-shift the atomic line centre so as to increase the scattering force of the blue-detuned beam, and thereby cause negative damping of the velocity. In the context of the velocity bunching observations noted earlier, this also produces a velocity feedback effect[14,15]. In the current system, the term $g(v)i_a$ markedly alters the dynamics, which would otherwise be that of an oscillator damped by the cooling beam (that is, $\kappa(v)i_c$). Indeed, the behaviour of this system, as now shown, is that of a Van der Pol oscillator[19,20]. As an aside, the Van der Pol oscillator equation is most often written with an amplification term containing quadratic saturation. Van der Pol, however, first introduced the amplification term as a function; and later Taylor-expanded this term about the operating point. The relevant functions in equation (1) could similarly be expanded to reveal a quadratic term, but have been left intact to preserve full generality of the results. For example, when $\Delta\omega_a = \gamma/\sqrt{3}$, the amplification in equation (1), to leading order, takes on the classic Van der Pol form given by $g(v)i_a \approx g(0)i_a - v^2/v_{sat}^2$, where

---

Max-Planck-Institut für Quantenoptik, 85748 Garching, Germany. *Permanent address: California Institute of Technology, Pasadena, California 91125, USA. †e-mail: vahala@caltech.edu; thu@mpq.mpg.de.
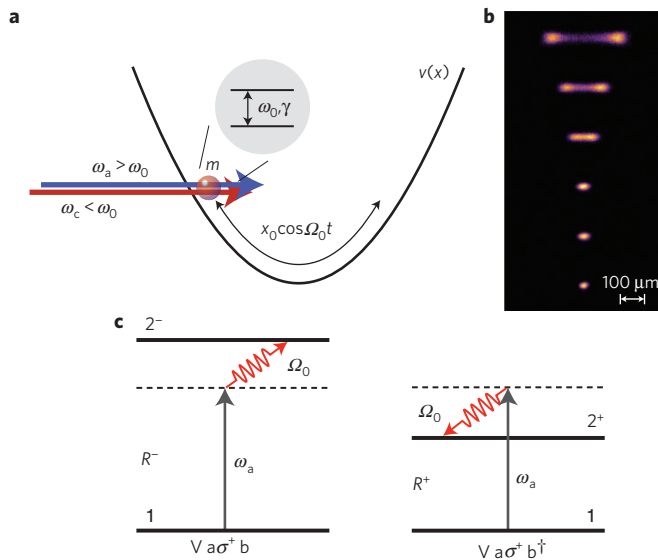
Figure 1 | Ion-trap illustration, observation of coherent motion and physical origin of stimulated phonon emission for the single-ion phonon laser. a, An ion in a harmonic trap interacting with a cooling beam (frequency ω_c) and an amplification beam (frequency ω_a). The ion with position x and mass m moves in a trap potential $v(x)$. The optical transition has frequency ω_0 and linewidth γ. **b**, Ion-luminescence series showing time-averaged motion. The amplification beam intensity is increasingly stepped from the lowest (no amplification) to upper images. The cooling beam intensity is constant. A threshold that marks a transition from thermal to coherent motion is apparent. **c**, At the quantum level, amplification results from net production of phonons through stimulated emission (rate R^+) and absorption (rate R^-) of centre-of-mass phonons. The corresponding, phonon-assisted transitions to the upper level are shown. Phonon emission and phonon absorptive transitions induce polarization at frequencies corresponding to levels 2^+ and 2^- in these diagrams. These lie within the distribution of transition frequencies given by the lineshape function. Analogies to stimulated Raman amplification are discussed in the text.

v_{sat}^{-2} is merely the second-order Taylor coefficient. The Van der Pol oscillator is commonly used to understand lasers and electronic oscillators[18,19]. It has a small-signal and large-signal (saturated) regime of operation; these are studied separately below.

Setting v to zero in the damping and amplification terms (small-signal regime), consider letting i_a increase from zero while holding i_c constant (fixed cooling). As i_a increases, ultimately, $g(0)i_a = \kappa(0)i_c$ (the threshold condition) at an intensity $i_a = i_T \equiv (\kappa(0)/g(0))i_c$. For $i_a > i_T$, the overall damping becomes negative in equation (1) (that is, $g(0)i_a > \kappa(0)i_c$), and ion motion grows, at first, exponentially in time; before finally stabilizing in the large-signal regime. Before considering this large-signal, saturation process, experimental observations of threshold are presented. A single, magnesium ion in a linear radiofrequency trap was studied. The experimental arrangement is nearly identical to that detailed in ref. 31. The Mg+D2 transition at 279.6 nm has a natural linewidth of 41.8 MHz and the axial secular frequency of the trap was set to 71 kHz in all measurements; micro-motion was negligible. The amplification beam was directed along the trap's long axis to excite only axial oscillations. The cooling beam was applied slightly off axis from the long axis so as to project onto all three axes of motion. Cooling to approximately 1 mK was obtained. Figure 1b shows a series of time-averaged images of the ion motion, for increasing levels of amplification beam intensity ($i_a = 0$ in the lowest image). A threshold at which the amplified, Brownian, thermal motion of the ion transitions to a double-lobed pattern (produced by
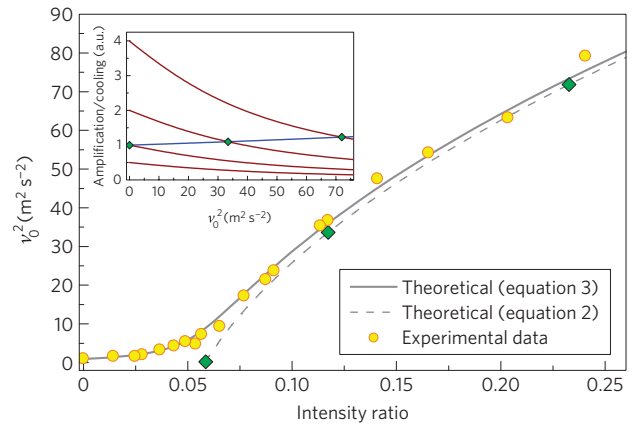
Figure 2 | A comparison of measured and predicted ion motion as a function of pumping that illustrates threshold behaviour and increasing coherent motion for pumping above threshold. Measured, square of ion-velocity amplitude (yellow, circles) plotted versus i_a/i_c (i_c held constant). Amplification/cooling beams are detuned by $+12$ MHz/-74 MHz. The solid curve is the steady-state solution of equation (3). To match the *ab initio* calculation, the data-set origin was shifted by (-0.05, -0.72 m^2 s^{-2}). Inset: The role of amplification saturation in establishing the operating point is illustrated by graphical solution of $G(v_0)i_a = K(v_0)i_c$ (steady-state solution of equation (2)). This excludes spontaneous emission since the Langevin force averages to zero. $G(v_0)i_a$ is plotted in red for beam intensities $i_a = 0.5, 1, 2, 4 \times i_T$, whereas $K(v_0)i_c$ is plotted in blue at a single cooling intensity (both are normalized to their threshold values, set equal to unity). For $i_a = i_T$, $G(0)i_T = K(0)i_c$ so that, trivially, $v_0 = 0$. However, with increasing amplification beam intensity, the point $v_0 = 0$ is no longer stable (that is, $G(0)i_a > K(0)i_c$ for $i_a > i_T$). In the terminology of laser oscillators, $G(0)i_a$ for $i_a > i_T$ is the unsaturated amplification. Saturation of the mechanical amplification restores balance of amplification with damping by increase of v_0 as illustrated. The corresponding operating points are diamonds, and are superimposed on the dashed curve (solution of $G(v_0)i_a = K(v_0)i_c$) in the main panel. The operating points are dynamically stable with respect to fluctuations as can be verified using the inset (perturbations create slight changes in net amplification/damping so as to restore the operating point).

the oscillatory motion of the ion) is apparent in the data. From these images, the velocity amplitude is determined using $v_0 = \Omega_0 x_0$; and the threshold behaviour is further apparent in Fig. 2 where the squared-velocity amplitude (to emphasize the threshold) is plotted versus i_a normalized by i_c. The ratio i_a/i_c is experimentally accessible, and, as discussed below, physically appropriate if, as was the case in this experiment, saturation of the atomic transition can be neglected. It was determined by measuring separately the ion luminescence induced by each beam at a reference, negative detuning. The amplification (cooling) beam detuning is set to $+12$ MHz (-74 MHz) in these measurements; and the solid curve in Fig. 2 is the theoretical operating point curve as discussed below.

The oscillator operating point (that is, amplitude of motion at a given pumping level) results from a saturation process, similar to amplification saturation in a Van der Pol oscillator (or laser oscillator). $\kappa(v)$ and $g(v)$, through their imbalance in the small-signal regime (that is, $g(0)i_a > \kappa(0)i_c$), cause growth in the amplitude of oscillation. Increases in motional amplitude induce saturation that restores the balance of amplification and damping. As in a Van der Pol oscillator and laser oscillator this balance occurs in a time-averaged sense over one cycle of motion. To analyse the saturation process, the velocity is expressed as $v = v_0\cos(\Omega_0 t + \phi)$, where v_0 and ϕ are a slowly varying amplitude and phase (that is, $\dot{v}_0 \ll \Omega v_0$ and $\dot{\phi} \ll \Omega_0$). On substitution of this expression into
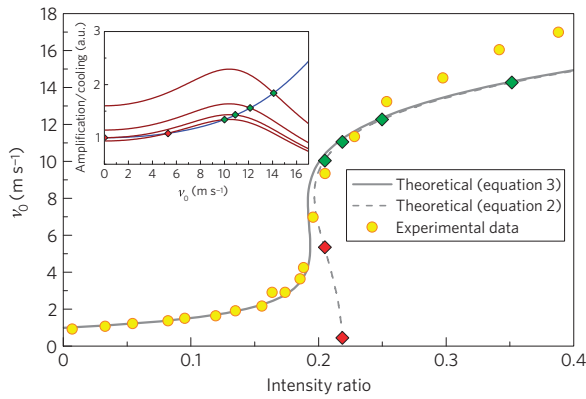
Figure 3 | A comparison of measured and predicted ion motion as a function of pumping that illustrates a regime of anomalous amplification saturation. Velocity amplitude data points in yellow plotted versus i_a/i_c for the amplification beam detuned by $+40$ MHz (that is, a regime of anomalous amplification saturation such that $\Delta\omega_a > \gamma/2$) and the cooling beam by -74 MHz. The solid curve is the steady-state solution of equation (3). For large intensity ratios, the oscillation amplitude becomes large compared with the beam waist of the cooling beam. As such, the data deviates from the predicted behaviour for larger amplitudes. As in Fig. 2, to match the *ab initio* calculation, the data-set origin was slightly shifted (in this case by $(0, -0.22\,\text{m s}^{-1})$). Inset: The role of anomalous saturation in creating operating point hysteresis is understood by graphical illustration of equation $G(v_0)i_a = K(v_0)i_c$ (steady-state solution of equation (2)). This excludes spontaneous emission since the Langevin force averages to zero. $G(v_0)i_a$ is plotted in red for four amplification beam intensities, whereas $K(v_0)i_c$ is plotted in blue at one cooling intensity (both are normalized to their threshold values, set equal to unity). Green (red) diamonds indicate corresponding dynamically stable (unstable) operating points, as per the caption of Fig. 2, and are superimposed on the dashed curve (solution of $G(v_0)i_a = K(v_0)i_c$) in the main panel. The shape of $G(v_0)i_a$ should be contrasted with that in Fig. 2, inset. In the present case, the gain saturation is anomalous, featuring, at first, a rising amplification with an increase of v_0.

equation (1) and keeping only leading-order terms,

$$\dot{v}_0 = -\frac{1}{2}[K(v_0)i_c - G(v_0)i_a]v_0 + \zeta(t) \qquad (2)$$

where $G(v_0)i_a$, $K(v_0)i_c$ and $\zeta(t)$ are the cycle-averaged amplification, damping and Langevin (both cooling and amplification beam related) force. Also useful is the dynamical equation for the cycle-averaged oscillator energy $E = mv_0^2/2$ (derived from equation (2)),

$$\dot{E} = -[K(E)i_c - G(E)i_a]E + S_a + S_c \qquad (3)$$

where $S_{c,a}$ is the mechanical power added by spontaneous emission; and damping and amplification are expressed here as functions of E. A detailed discussion of equations (2) and (3), as well as closed-form expressions for K, G and $S_{c,a}$, is provided in the Supplementary Information.

The steady-state solutions to equations (2) and (3) provide operating point equations for amplitude (v_0) and energy, or equivalently v_0^2 (note: a dynamic stability condition is also necessary as discussed in the caption of Fig. 2). As the optical transition is assumed to be only weakly saturated, i_a and i_c factor from the terms $S_{c,a}$. By dividing through by i_c in the steady state of equations (2) and (3), the operating point functions take the form $v_0(i_a/i_c)$ and $v_0^2(i_a/i_c)$. They are plotted in Fig. 2 using independently measured parameters (that is, secular oscillation frequency and amplification/cooling beam frequency detuning). To match the *ab initio* calculations the

measured data sets were shifted slightly (see Figs 2 and 3 captions) to compensate for imperfect calibration of the coordinate origin. The resulting agreement is excellent. As the combined effect of imaging system resolution and thermal motion makes it difficult to distinguish the stochastic (that is, thermal) and coherent contributions to motion at the lowest amplitudes, the overall agreement with data is better using the energy operating point equation (solid grey curve), which essentially gives the variance of motion.

Both theory and experiment show that the studied system has striking analogies to an optical laser. As a function of the amplification beam intensity (pumping level), it features a threshold for transition from thermal motion to self-sustained, stable oscillations. The physical connection is, in fact, deeper; and, as now shown, the coherent oscillations are sustained by stimulated generation of phonons. In the Lamb–Dicke regime (effectively, the small-signal-regime limit of the Hamiltonian), the interaction is $H_I = Va\sigma^+(b+b^\dagger) + \text{h.a.}$ (ref. 33), where $V \equiv \hbar\Omega_R k\sqrt{\hbar/8m\Omega_0}$ (Ω_R is the vacuum Rabi frequency, $k \equiv \omega_0/c$ and m is the ion mass), b (a) is the phonon (photon) destruction operator and σ^+ is the two-level Pauli raising operator. Two, distinct processes are illustrated in Fig. 1c: one in which a centre-of-mass phonon is created and the second in which it is destroyed. As the optical transition frequency is itself a distribution of frequencies given by the transition lineshape function $f_\gamma(\omega - \omega_0)$ (defined to be unity at $\omega = \omega_0$), the corresponding transition rates can be found in the standard way using Fermi's golden rule[34],

$$R^+ = \beta f_\gamma(\Delta\omega_a - \Omega_0)(n+1) \qquad (4)$$

$$R^- = \beta f_\gamma(\Delta\omega_a + \Omega_0)n \qquad (5)$$

where $R^\pm$ are the transition rates for creation $(+)$ and destruction $(-)$ of a phonon; and $\beta \equiv \hbar k^2\gamma\, i_a/4m\Omega_0 i_{sat}$, where i_{sat} is the saturation intensity of the dipole transition. In addition, as optical saturation of the transition is assumed to be weak ($i_a \ll i_{sat}$), negligible occupancy of the upper atomic level is assumed. Significantly, the creation rate R^+ has two components: a stimulated part that is proportional to the number of vibrational quanta, n, and a spontaneous part. In the sideband-resolved regime, the relevant rate equation for phonon number is given by,

$$\dot{n} = (R^+ - R^-) = \beta[f_\gamma(\Delta\omega_a - \Omega_0) - f_\gamma(\Delta\omega_a + \Omega_0)]n + s \qquad (6)$$

where equations (4) and (5) have been used and $s \equiv \beta f_\gamma(\Delta\omega_a - \Omega_0)$ is the spontaneous generation rate of phonons from equation (4). The coefficient of 'n' in equation (6) is the phonon amplification for the case of sideband-resolved operation. This case can be used to establish that stimulated emission is also responsible for the observed amplification in the present, unresolved-sideband case. To verify this, consider the net rate of phonon generation, $R^+ - R^-$, in the weak-binding limit:

$$\lim_{\Omega_0 \to 0}(R^+ - R^-) = g(0)i_a n + s = G(0)i_a n + s \qquad (7)$$

where to establish equality, the formula for $g(0)$ and also $G(0) = g(0)$ (both given in the Supplementary Information) have been used here. Equation (7) shows that amplification in equation (1) and in equation (3) is the result of stimulated emission of phonons. The ion oscillator therefore constitutes the mechanical equivalent of a laser; or a phonon laser.

The ion phonon laser operates with no identifiable inversion, and, in this sense, resembles a Raman laser. Indeed, an analogy

with stimulated Raman emission can be drawn by allowing the polarization between 2^+ and 1 (that is, the operator σ^+) in Fig. 1c (right) to have the role of the Stokes wave. Stimulated Raman emission relies on damping of the phonon field that is much greater than for that of the optical Stokes field[35]. In the present situation, on account of the weak-binding assumption, it is instead the polarization (that is, effectively the Stokes field) that is more strongly damped than the phonon field. In such a case, it is the phonon field that will experience stimulated amplification[35]. A rigorous analysis shows that this is the case, and reconfirms the above expression based on Fermi's golden rule.

The above arguments, which provide an expression for the un-saturated amplification (that is, the small-signal regime), also give physical insight into how the mechanical amplification saturates within the ion system. From equation (7), $g(0)$ is proportional to the competing phonon emission and absorption rates, and, in the weak-binding limit, this difference is proportional to the slope of the lineshape function evaluated at the pumping frequency. The large-signal analysis provided in the Supplementary Information shows that this slope continues to figure prominently, but in a time-averaged sense. In particular, in the weak-binding limit, the large-signal interaction Hamiltonian can be shown to yield an absorption spectrum for the ion in motion that is merely the Doppler-shifted lineshape function[33]. Under coherent motion, the ion therefore presents a time-varying line centre, and hence lineshape slope, at the pumping frequency. The analysis shows that a properly weighted time-averaged slope over one cycle of motion yields the function $G(\nu_0)$. Saturation thereby can be interpreted to result as a variation in this time-averaged slope with increasing motional amplitude.

Considerable attention has been focused on solid-state implementations of phonon lasers. In these systems, the low velocity of sound in solids presents a challenge to realization of phonon laser action through the accompanying high density of phonon states. This shortens lifetimes by creating transitions that compete directly with the phonon laser transition[25]. Indeed, engineering vibronic band structure has been proposed to restrict vibronic coupling[25]. In this sense, a single, trapped ion represents a limit of zero vibronic coupling that would be possible using a quasi-zero-dimensional vibronic band structure (that is, delta-function phononic density of states). Ion systems have a further intriguing property in that vibronic modes can be controllably added through the introduction of more ions to the trap. Such ion chains and their normal modes are well established in the application of ions to quantum computing[2]. In phonon lasers, they can, in principle, provide a highly controlled way to study the transition away from the zero-dimensional system. Moreover, as shown in the present work, ion systems feature independently controlled damping and amplification beams. As a result, the initial (un-amplified) mechanical Q factor of the system can be adjusted through control of the red-detuned pumping intensity. The independent control of power and tuning for this beam and the amplification beam also creates other intriguing dynamical regimes as noted below.

Several distinct regimes of mechanical amplification saturation exist in this system. The regime of Fig. 2 occurs for $0 < \Delta\omega_a < \gamma/2$. For these detuning values, the amplification function, $G(\nu_0)i_a$, will monotonically decrease with increased motional amplitude (Fig. 2, inset). This is normal saturation, typical of saturation behaviour in a laser oscillator[19]. However, when $\Delta\omega_a > \gamma/2$, the behaviour alters markedly. In this case, the amplification function initially rises with increasing oscillator amplitude, before finally decreasing at large amplitudes. This anomalous behaviour creates hysteresis in the operating point and is considered in Fig. 3. Hysteretic behaviour, as noted in the introduction, was observed previously for different experimental conditions (a single laser, trap stiffness was varied) and modelled on the basis of heating[13]. Concerning yet other regimes, the damping rate associated with the cooling beam also

undergoes saturation, and can affect the stability of the ion system. The analysis and experimental data presented here have featured a large cooling-beam detuning (compared with the full-width at half-maximum of the transmission) that is also larger than the gain beam detuning (that is, $|\Delta\omega_c| > \Delta\omega_a$). A wider range of behaviours is expected when either of these conditions changes, and will be taken up in a future experimental study.

A phonon laser has been demonstrated by optical pumping of a trapped ion. The optomechanical interaction associated with the scattering force gives rise to a Van der Pol dynamical system in which amplification is provided by stimulated emission of centre-of-mass phonons. Steady-state operation occurs by saturation of the mechanical amplification, and excellent agreement is obtained between theory and observed mechanical motion versus pumping. The ability to locate microscopic sources of vibrational coherence that are optically driven and cooled (and addressable using wavelength) might provide a new tool in the field of trapped-ion physics. The fact that phonon laser action is sustained by very low power levels suggests that the ion might be used as an ultra-sensitive force probe. Moreover, amplification of the centre-of-mass motion[36] is potentially useful in its own right. The single ion, as a class of phonon laser, represents a kind of zero-dimensional limit in which there is no vibronic output coupling. In a Fabry–Perot laser analogy, the mirrors would be 100% reflecting and threshold would be determined by internal cavity losses. At the same time, however, this does not preclude other types of useful coupling to the ion's vibrational motion (such as electromagnetic). For example, successful injection locking of the ion phonon laser, in analogy to slaving of a laser oscillator by an external master oscillator, has been achieved recently and will be reported elsewhere.

Note added in proof. After submission of this paper, a related theory of an optically pumped ion as a motional oscillator was reported by A. E. Kaplan[37].

References

1. Kimble, H. J. The quantum internet. *Nature* **453,** 1023–1030 (2008).
2. Blatt, R. & Wineland, D. Entangled states of trapped atomic ions. *Nature* **453,** 1008–1015 (2008).
3. Helmerson, K. & Phillips, W. D. Cooling, trapping and manipulation of atoms and Bose–Einstein condensates: Applications to metrology. *Riv. Nuovo Cimento* **31,** 141–186 (2008).
4. Bloch, I. Quantum coherence and entanglement with ultracold atoms in optical lattices. *Nature* **453,** 1016–1022 (2008).
5. Cohen-Tannoudji, C. N. Manipulating atoms with photons. *Rev. Mod. Phys.* **70,** 707–719 (1998).
6. Hänsch, T. W. & Schawlow, A. L. Cooling of gases by laser radiation. *Opt. Commun.* **13,** 68–69 (1975).
7. Wineland, D. & Dehmelt, H. Proposed 1014 delta upsilon less than upsilon laser fluorescence spectroscopy on t1+ mono-ion oscillator iii. *Bull. Am. Phys. Soc.* **20,** 637–637 (1975).
8. Wineland, D. J., Drullinger, R. E. & Walls, F. L. Radiation pressure cooling of bound resonant absorbers. *Phys. Rev. Lett.* **40,** 1639–1642 (1978).
9. Neuhauser, W., Hohenstatt, M., Toschek, P. & Dehmelt, H. G. Optical-sideband cooling of visible atom cloud confined in parabolic well. *Phys. Rev. Lett.* **41,** 233–236 (1978).
10. Wineland, D. J. & Itano, W. M. Laser cooling of atoms. *Phys. Rev. A* **20,** 1521–1540 (1979).
11. Javanainen, J. *Fundamentals of Laser Interactions: Proceedings of a Seminar Held at Obergurgl, Austria, February 24–March 2* Vol. 229, 249–258 (Springer, 1985).
12. Sauter, T., Gilhaus, H., Neuhauser, W., Blatt, R. & Toschek, P. Kinetics of a single trapped ion—multistability and stimulated 2-photon light force. *Europhys. Lett.* **7,** 317–322 (1988).
13. Quint, W. *Chaos und Ordnung von Lasergekühlten Ionen in einer Paul-Falle.* PhD thesis, Ludwig Maximillians Univ. (1990).
14. Loftus, T. H., Ido, T., Ludlow, A. D., Boyd, M. M. & Ye, J. Narrow line cooling: Finite photon recoil dynamics. *Phys. Rev. Lett.* **93,** 073003 (2004).
15. Loftus, T. H., Ido, T., Boyd, M. M., Ludlow, A. D. & Ye, J. Narrow line cooling and momentum-space crystals. *Phys. Rev. A* **70,** 063413 (2004).

16. Kippenberg, T. J. & Vahala, K. J. Cavity optomechanics: Back-action at the mesoscale. *Science* **321,** 1172–1176 (2008).
17. Kippenberg, T. J. & Vahala, K. J. Cavity opto-mechanics. *Opt. Express* **15,** 17172–17205 (2007).
18. Yariv, A. *Quantum Electronics* 307–309 (Wiley, 1975).
19. Sargent, M., Scully, M. O. & Lamb, W. E. *Laser Physics* 45–54 (Addison-Wesley, 1974).
20. Van der Pol, B. A theory of the amplitude of free and forced triode vibrations. *Radio Rev.* **1,** 701–710 (1920).
21. Wallentowitz, S., Vogel, W., Siemers, I. & Toschek, P. E. Vibrational amplification by stimulated emission of radiation. *Phys. Rev. A* **54,** 943–946 (1996).
22. Liu, H. C. *et al.* Coupled electron–phonon modes in optically pumped resonant intersubband lasers. *Phys. Rev. Lett.* **90,** 077402 (2003).
23. Bargatin, I. & Roukes, M. L. Nanomechanical analog of a laser: Amplification of mechanical oscillations by stimulated Zeeman transitions. *Phys. Rev. Lett.* **91,** 138302 (2003).
24. Chudnovsky, E. M. & Garanin, D. A. Phonon superradiance and phonon laser effect in nanomagnets. *Phys. Rev. Lett.* **93,** 257205 (2004).
25. Chen, J. & Khurgin, J. B. Feasibility analysis of phonon lasers. *IEEE J. Quantum Electron.* **39,** 600–607 (2003).
26. Tucker, E. B. Amplification of 9.3-kMc/sec ultrasonic pulses by maser action in ruby. *Phys. Rev. Lett.* **6,** 547–547 (1961).
27. Hu, P. Stimulated emission of 29-cm^{-1} phonons in ruby. *Phys. Rev. Lett.* **44,** 417–420 (1980).
28. Fokker, P. A., Dijkhuis, J. I. & deWijn, H. W. Stimulated emission of phonons in an acoustical cavity. *Phys. Rev. B* **55,** 2925–2933 (1997).
29. Bron, W. E. & Grill, W. Stimulated phonon emission. *Phys. Rev. Lett.* **40,** 1459–1463 (1978).
30. Kent, A. J. *et al.* Acoustic phonon emission from a weakly coupled superlattice under vertical electron transport: Observation of phonon resonance. *Phys. Rev. Lett.* **96,** 215504 (2006).
31. Herrmann, M. *et al.* Frequency metrology on single trapped ions in the weak binding limit: The 3s(1/2)–3p(3/2) transition in Mg-24(+). *Phys. Rev. Lett.* **102,** 1–4 (2009).
32. Paul, W. Electromagnetic traps for charged and neutral particles. *Rev. Mod. Phys.* **62,** 531–540 (1990).
33. Leibfried, D., Blatt, R., Monroe, C. & Wineland, D. Quantum dynamics of single trapped ions. *Rev. Mod. Phys.* **75,** 281–324 (2003).
34. Yariv, A. *Quantum Electronics* 56–57 (Wiley, 1975).
35. Shen, Y. R. & Bloembergen, N. Theory of stimulated Brillouin and Raman scattering. *Phys. Rev.* **137,** 1787–1805 (1964).
36. Dehmelt, H., Nagourney, W. & Sandberg, J. Self-excited mono-ion oscillator. *Proc. Natl Acad. Sci. USA* **83,** 5761–5763 (1986).
37. Kaplan, A. E. Single-particle motional oscillator powered by laser. *Opt. Express* **17,** 10035–10043 (2009).

Author contributions

M.H., S.K., V.B. and G.S. carried out measurements. K.V., M.H. and Th.U. carried out simulations. K.V., M.H., Th.U. and T.W.H. developed the concepts. All authors worked together to plan the measurements and write the manuscript.

Additional information

Supplementary information accompanies this paper on www.nature.com/naturephysics. Reprints and permissions information is available online at http://npg.nature.com/reprintsandpermissions. Correspondence and requests for materials should be addressed to K.V. or Th.U.